Collection de notes internes de la Direction des Etudes et Recherches

DETERMINATION DES CONTRAINTES INTERNES DANS UN ACIER INOXYDABLE AUSTENOFERRITIQUE

INTERNAL STRESSES IN AN AUSTENOFERRITIC DUPLEX STAINLESS STEEL

EDF
Electricité de France

EDF
Electricité de France

Direction des Etudes et Recherches

SERVICE RÉACTEURS NUCLÉAIRES ET ECHANGEURS
Département Etude des Matériaux

Avril 1996

VERHAEGHE B.
BRECHET Y.
LOUCHET F.
MASSOUD J.P.
TOUZEAU D.

DETERMINATION DES CONTRAINTES INTERNES DANS UN ACIER INOXYDABLE AUSTENOFERRITIQUE

INTERNAL STRESSES IN AN AUSTENOFERRITIC DUPLEX STAINLESS STEEL

Pages : 14

96NB00143

Diffusion : J.-M. Lecœuvre
EDF-DER
Service IPN. Département SID
1, avenue du Général-de-Gaulle
92141 Clamart Cedex

ISSN 1161-0611

SYNTHÈSE :

Les aciers austénoferritiques biphasés contiennent une phase dure et une phase molle en proportion comparable, les deux phases sont bipercolées. Ces aciers sont donc susceptibles de développer des contraintes internes importantes quand ils sont déformés. L'évolution et la relaxation de ces contraintes, ainsi que l'endommagement du matériau ont été caractérisés à l'aide d'essais Bauschinger.

Nous avons comparé le comportement du matériau vieilli thermiquement à celui du non vieilli. Les contraintes internes ont été efficacement relaxées par la déformation plastique de la phase dure.

EXECUTIVE SUMMARY :

Austenoferritic duplex steels possess microstructures containing comparable volume fractions of hard and soft phases which are bipercolated. They are therefore liable to develop large internal stresses during straining. The evolution and the relaxation of these stresses and the occurrence of damage are characterized using Bauschinger tests.

Thermally aged and non-aged material behaviour are compared. Plastic flow in the hard phase is shown to be significantly efficient in releaving these internal stresses.

LTPCM/ENSEEG, Saint Martin d'Hères[1]) *(a) and*
EDF, Moret-sur-Loing[2]) *(b)*

Internal Stresses in an Austenoferritic Duplex Stainless Steel

By

B. VERHAEGHE (a), Y. BRECHET (a), F. LOUCHET (a), J. P. MASSOUD (b), and D. Touzeau (b)

1. Introduction

A number of two-phase alloys, like austenoferritic duplex stainless steels, develop internal long-range stresses when they are plastically deformed [1, 2]. Internal stresses have a strong effect on the mechanical properties of these alloys such as work hardening behaviour or damage [1, 3]. The origin of polarized internal stresses in such materials are the deformation incompatibilities between the two phases. Those incompatibilities can be of elastic nature (if the Young moduli of the two phases are different) or of plastic nature (if the yield stresses are different). In the case of duplex stainless steels, the austenitic and ferritic phases have roughly the same Young modulus but very different yield stresses, therefore the incompatibilities are essentially of plastic origin: one phase plastically deforms while the other remains elastic. This heterogeneity of plastic deformation leads to polarized internal stresses which will be labelled σ_i.

Bauschinger tests are a simple way to measure σ_i [4, 5]. The Bauschinger effect is the difference in yield stress after deformation reversal [6]. It results from the directionality of σ_i. Polarized internal stresses oppose the applied stress which was at their origin but help the deformation when the strain is reversed. Moreover the Bauschinger effect may be sensitive to damage processes [7].

[1]) Domaine Universitaire, F-38402 Saint Martin d'Hères, France.
[2]) Les Renardières, Route de Sens, F-77250 Moret-sur-Loing, France.

It is useful to study the Bauschinger effect in duplex stainless steels for two different reasons. First the yield stress of the ferrite varies during thermal ageing. Secondly, the material has a specific microstructure in that the two phases are percolated. Whereas experimental investigation and modelling of internal stresses for particle reinforced materials or fibrous structures is well developed [6, 8, 9] there is comparatively little work done on complex structures. Austenoferritic stainless steels are in a way a model system for these problems as they are bipercolated, the volume fractions are of the same order of magnitude, and the ferrite/austenite interface is expected to be strong.

The purpose of this work is to investigate the building up of internal stresses with plastic straining through quantitative analysis of the Bauschinger effect. The occurrence of damage or plastic flow in the hard phase and its influence on Bauschinger effect will also be investigated.

2. Principles of the Method

If a specimen undergoes a strain ε_T, the flow stress σ_F can be written as

$$\sigma_F = \sigma_0 + \sigma_f + \sigma_i , \tag{1}$$

where $\sigma_f + \sigma_i$ is the work hardening increment, σ_f (forest hardening) is the non-directional contribution to work hardening of the plastic phase, σ_0 is the intrinsic yield stress of the matrix, and σ_i the long-range stresses due to incompatibilities.

If, after prestraining, the direction of the applied stress is reversed, the internal stresses will promote the onset of reversed plastic deformation and the reversed yield stress will be given by

$$\sigma_R = \sigma_0 + \sigma_f - \sigma_i . \tag{2}$$

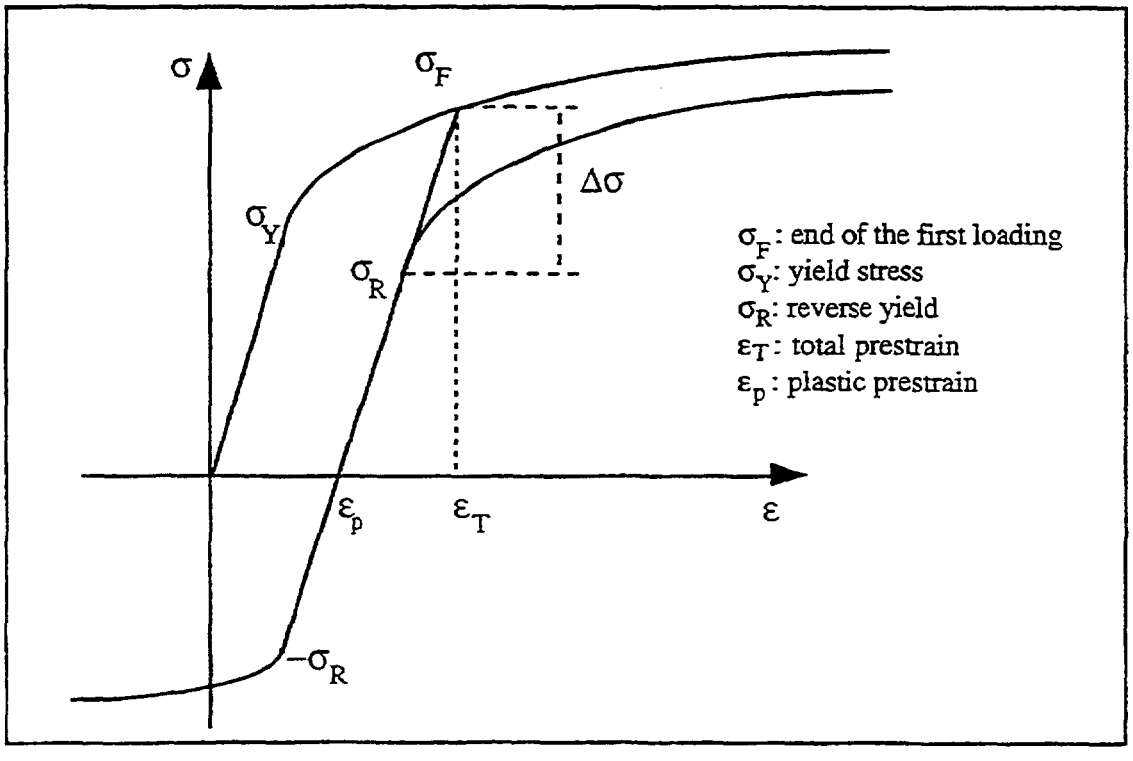

Fig. 1. Features of the Bauschinger effect

Combining (1) and (2) leads to

$$\sigma_i = \tfrac{1}{2}(\sigma_F - \sigma_R) \tag{3}$$

provided that σ_F and σ_i values during forward and reverse straining are stable [5]. This very simple approach relates internal stresses to the Bauschinger effect.

The Bauschinger effect will be large in two-phase alloys containing a large volume fraction of a second phase with a high yield stress.

In the present study the internal stresses were calculated using equation (3). To evaluate the yield-lowering effect of the Bauschinger effect, we used the Bauschinger stress parameter β_σ [6], with the conventions defined on Fig. 1,

$$\beta_\sigma = \frac{\Delta\sigma}{\sigma_F}, \tag{4}$$

where $\Delta\sigma$ is the yield stress reduction, σ_F is the flow stress where the strain is reversed, $-\sigma_R$ is the reverse yield stress. Equation (4) can be written as

$$\beta_\sigma = 1 - \frac{\sigma_R}{\sigma_F}. \tag{5}$$

In the absence of the Bauschinger effect, $\sigma_R = \sigma_F$ and $\beta_\sigma = 0$. If β_σ exceeds unity, the Bauschinger effect is extremely large: reverse yielding occurs before the reverse stress is applied, this is sometimes observed in metal–matrix composites [10]. Generally $0 < \beta_\sigma < 1$.

3. Materials and Experimental Procedure

The materials studied are two cast austenoferritic duplex stainless steels (CC and EL) with neighbouring compositions (Table 1). They were solution-treated at 1120 °C for 6 h and quenched in water. Then, some of them were aged at 400 °C (Table 2).

Austenoferritic duplex stainless steels are known to embrittle after long-term ageing at 400 °C, which can affect the mechanical properties [11 to 13]. The properties of the austenite are not affected, but conversely the ferrite hardness and its microstructure continuously evolve during ageing. Below 500 °C, the unmixing by spinodal decomposition of the δ-Fe–Cr solid solution leads to the formation of a Cr-rich α′-phase ("475 °C embrittlement") sometimes accompanied by the precipitation of a Ni, Si, Mo-rich G-phase [14, 15].

Table 1
Chemical composition (wt%) and ferrite content (%) of duplex stainless steels

	C	P	Si	Mn	Ni	Cr	Mo	N	Nb	ferrite
EL	0.027	0.023	1.13	1.03	10.00	21.70	2.72	0.039	0.15	33
CC	0.038	0.027	1.20	0.71	10.43	22.11	2.75	0.042	0.21	33

Table 2
Ageing treatment of CC and EL

CC0	CC7	EL8
non-aged	aged 1000 h at 400 °C	aged 3000 h at 400 °C

Table 3
Yield stress of ferrite and austenite before and after ageing estimated by ultramicrohardness

before ageing		after ageing	
ferrite	austenite	ferrite	austenite
≈400 MPa	≈200 MPa	≈600 MPa	≈200 MPa

The CC7 and EL8 heat treatments have reached the same degree of embrittlement (lower-bound values of impact energy with ageing time). The embrittlement is associated with an increase of the yield stress of these alloys, due to the increase of the yield stress of the ferrite phase (Table 3). The yield stresses of each phase were estimated by ultramicrohardness measurements which were performed. The ultramicrohardness technique consists of multiple indentation cycles at the same location of a polished surface by a spherical indenter (10 μm radius ball indenter). Each cycle contains indentation, unload, and reload sequences. Automation of the test allows to obtain all values of each cycle directly in strength versus penetration depth. When plastic deformation largely overwhelms elastic deformation, the results can be converted in stress versus strain curves. The values of the yield stress can then be deduced by extrapolation.

Another consequence of ageing is the evolution of the fracture mechanisms. The non-aged samples fail in a ductile way in both phases. The plastic deformation of the two phases was observed to be homogeneous both by TEM (transmission electron microscopy) and by "in situ" SEM (scanning electron microscopy). In contrast, in the aged materials the ferrite fails by cleavage while the austenite remains ductile. In addition to cleavage, localized glide and perhaps also twinning occur in the ferrite phase.

With different plastic properties between the two phases and a large proportion of hard ferrite phase, austenoferritic steels and mainly the aged ones are expected to exhibit a high Bauschinger effect.

The Bauschinger tests were performed at EDF research centre on a Mayes cyclic machine. The Bauschinger effect was measured using separate samples (to avoid problems related to work hardening) after a total deformation $\varepsilon_T = 0.35\%$, 1%, 2%, 3% for CC0,

Table 4
σ_i and β_σ for CC0, CC7, and EL8 at different plastic strains. T–C: first loading in tension, C–T: first loading in compression

	CC0			CC7			EL8		
	ε_p (%)	σ_i (MPa)	β_σ	ε_p (%)	σ_i (MPa)	β_σ	ε_p (%)	σ_i (MPa)	β_σ
T–C	0.18	234	1.39	0.176	233	1.27	0.025	79	0.66
tests	0.88	323	1.45	0.252	284	1.36	0.272	286	1.36
	1.76	337	1.42	0.315	307	1.42	0.588	490	1.54
	2.74	350	1.43	0.45	385.5	1.5	1.62	534.5	1.61
				0.86*)	524	1.67	2.64	587	1.64
C–T				0.188	246.5	1.26			
tests				0.465	368	1.43			

*) Sample already deformed at $\varepsilon_p = 0.176\%$.

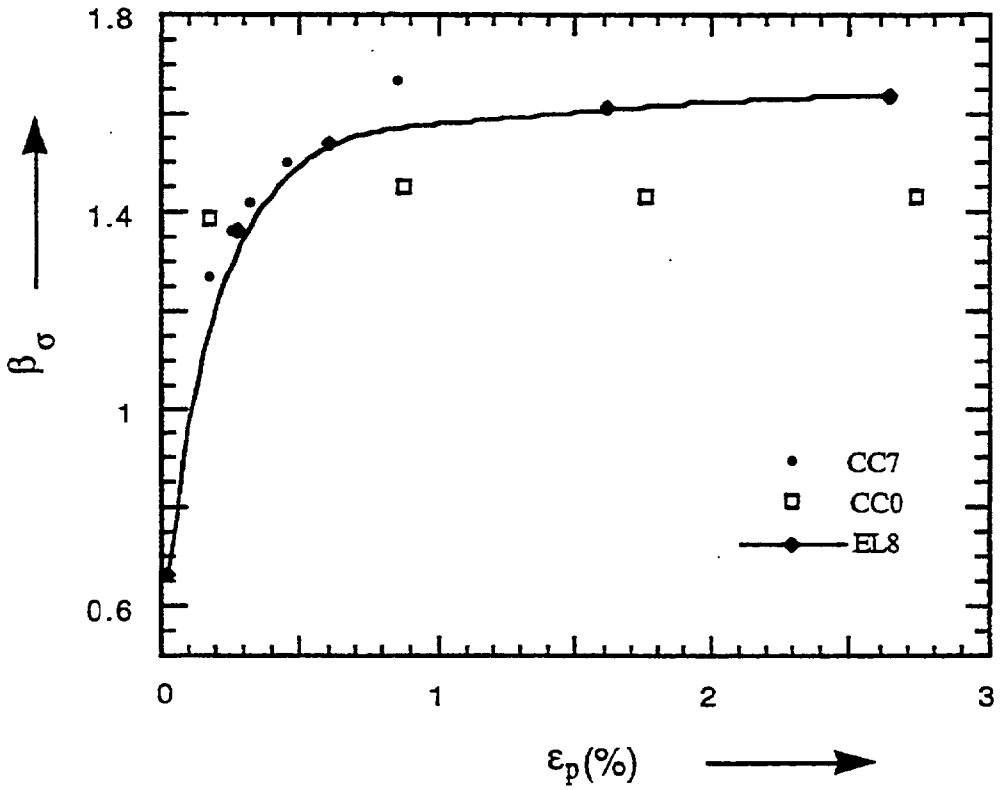

Fig. 2. Bauschinger stress parameter variation with ε_p for CC7, CC0, and EL8 alloys

$\varepsilon_T = 0.35\%, 0.45\%, 0.55\%, 0.73\%, 1.2\%$ for CC7, and $\varepsilon_T = 0.15\%, 0.5\%, 1\%, 2\%, 3\%$ for EL8. The first loading was in tension. For two tests with the CC7 material at $\varepsilon_T = 0.35\%$ and 0.73%, the first loading was in compression.

4. Results

As austenite is the soft phase, it is considered here as the matrix, even if, from a microstructural genesis point of view, the austenite grew out of the ferrite phase by solid state transformation. The resulting geometry is in fact bipercolated. The values of σ_i in the austenite phase and of β_σ are given in Table 4 for different ε_p (plastic prestrain). Fig. 2 and 3 represent, respectively, $\beta_\sigma = f(\varepsilon_p)$ and $\sigma_i = f(\varepsilon_p)$.

5. Discussion

5.1 Internal stresses in austenite

Pre-existing internal stresses (at $\varepsilon_p = 0$) are of the order of 60 MPa. As expected the Bauschinger effect is important for all the heat treatments. For $\varepsilon_p > 0.15\%$ (EL8 material, Fig. 2) plastic deformation already occurs during unloading (i.e. $\beta_\sigma > 1$) which is the sign of extremely large internal stresses. Austenite internal stresses rapidly increase with increasing ε_p (Fig. 3) up to a value ε_p after which they reach a relatively stable stage. The change in slope is around $\varepsilon_p = 0.5\%$ for both CC0 and aged materials.

For CC0, as it was not possible to reveal plastic deformation in sections of deformed samples by etching, "in situ" tensile tests in the scanning electron microscope were performed. Plastic deformation was observed to occur first in the austenite and to begin in ferrite at about 0.5% of plastic deformation. Ferrite deforms homogeneously before failure

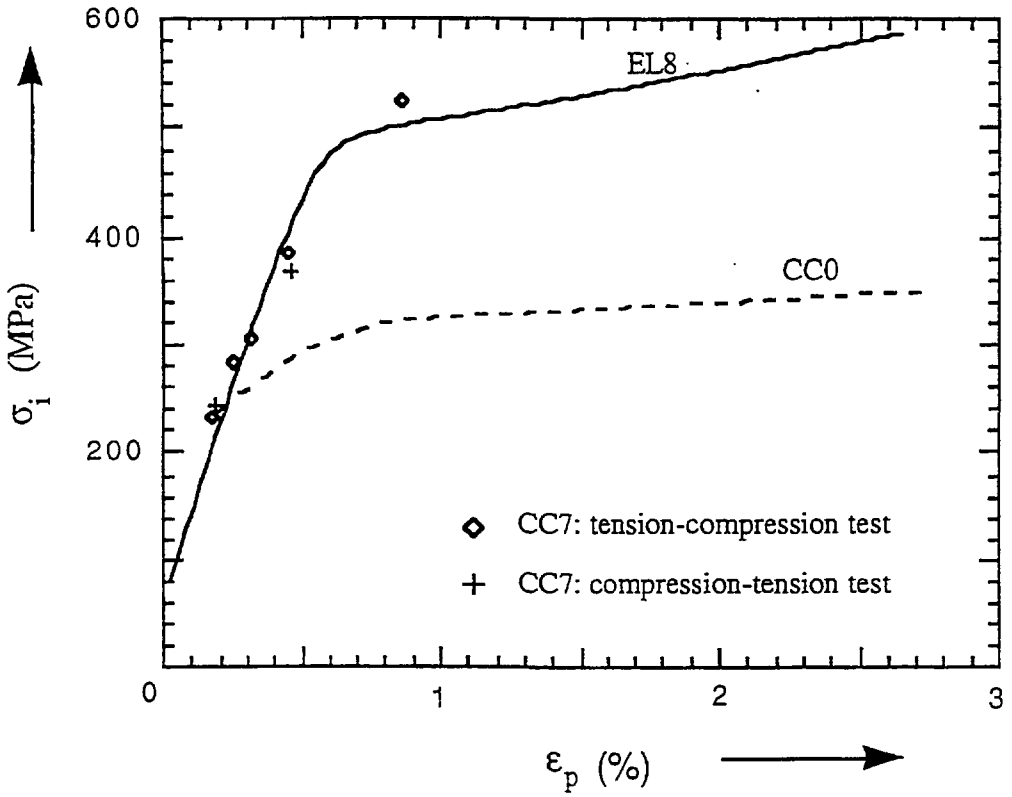

Fig. 3. Variation of internal stresses with ε_p in austenite of CC7, CC0, and EL8 alloys

of the sample (Fig. 4). Above this strain, internal stresses are relaxed by plastic homogeneous deformation of the ferrite phase.

For aged materials, the relaxation of the ferrite phase can occur in principle by cleavage, localized glide, and occasional twinning. Optical micrographs of longitudinal sections of Bauschinger samples (polished and electrochemically etched with an oxalic acid solution) show that cleavage cracks occur in the early stages of deformation, before glide appears in the ferrite (Fig. 5). The sudden change of slope in the internal stress–

Fig. 4. "In situ" SEM tensile test of CC0 sample, homogeneous deformation of the two phases

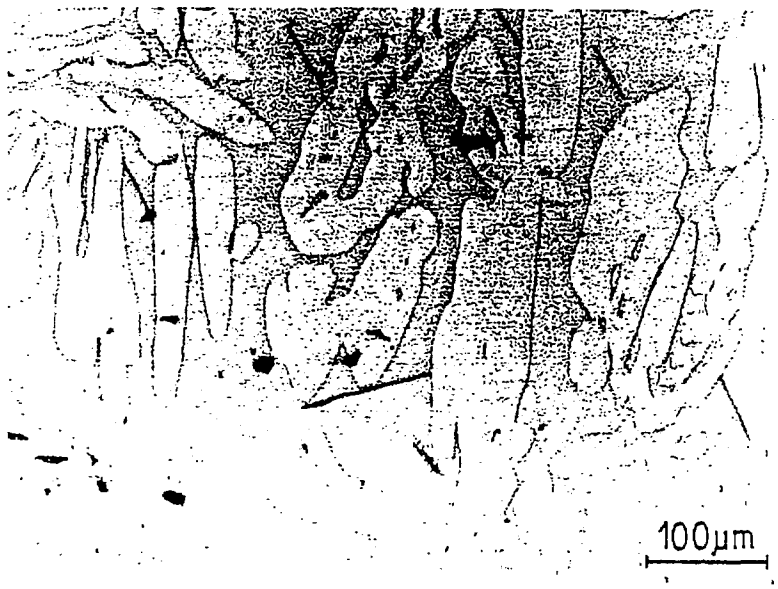

Fig. 5. Cleavage cracks in the ferrite phase, cracks occurring during tensile loading are perpendicular to the tensile axis (the tensile axis is parallel to the horizontal side of the picture), compression cracks are parallel. CC7 sample deformed at $\varepsilon_p = 0.25\%$

strain curves corresponds to the generalization of the localized glide in ferrite (Fig. 6). There is no evidence of twins in these Bauschinger samples. It is surprising to notice that in spite of early cleavage events, relaxation of internal stresses is essentially due to this localized glide. However cleavage cannot relax stresses efficiently enough without interfacial decohesions. Due to the strength of the austenite–ferrite interphase, the ferrite skeleton continues to support most of the external load and to participate in stress accumulation, even if cleavage cracks arise. This is indeed the reason why a same ferrite island can have multiple cracks (Fig. 7). One can notice in addition that the slope corresponding to stress accumulation for CC0 material after the beginning of plastic homogeneous deformation is lower than that for localized glide of aged materials.

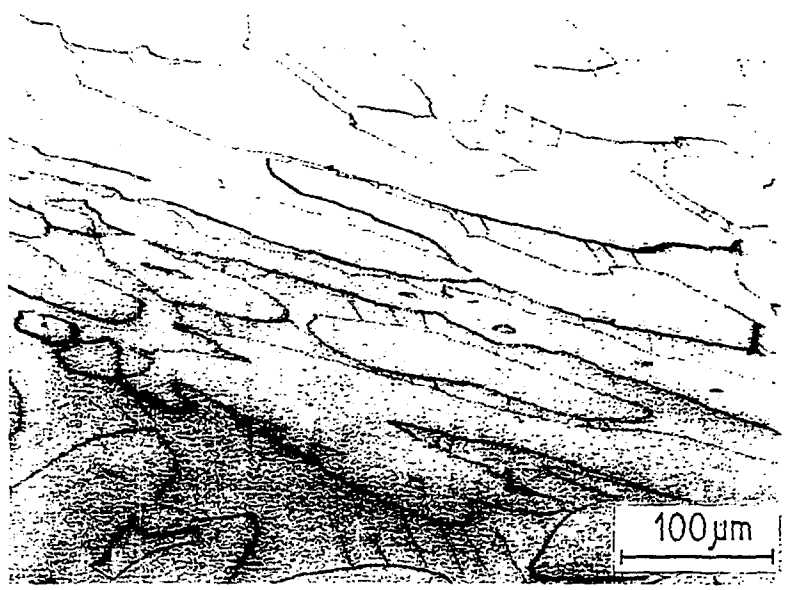

Fig. 6. Glide in the ferrite phase of the EL8 sample deformed at $\varepsilon_p = 0.59\%$. The chemical etching does not reveal the glide in the austenite phase

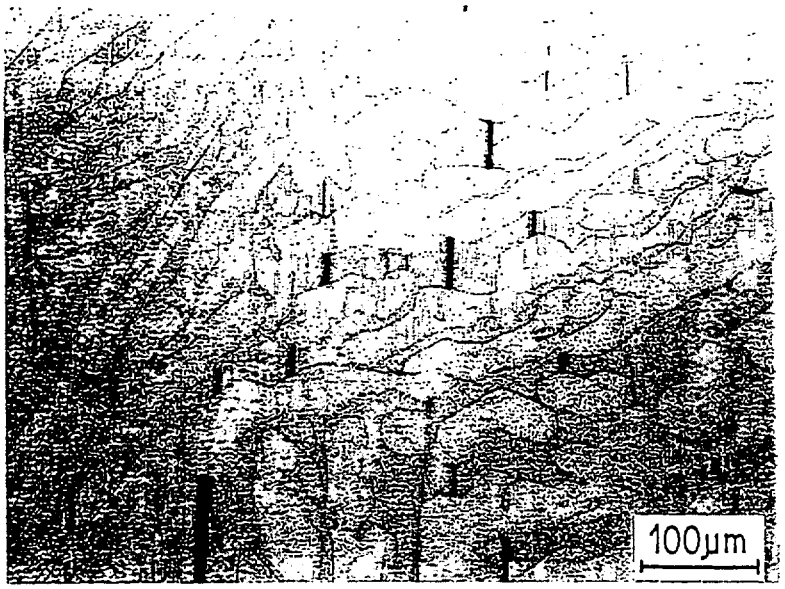

Fig. 7. Multiple cracks in the same ferrite islands. EL8 sample deformed at $\varepsilon_p = 2.85\%$

5.2 *Theoretical slope of* $\sigma_i = f(\varepsilon_p)$

For relatively small values of ε_p the internal stresses in the matrix can be estimated from Eshelby-type calculations developed by Brown and Clarke [8],

$$\sigma_i = 2\gamma\mu f\varepsilon_p\,; \tag{6}$$

$\mu = (3/8)\,E \approx 75$ GPa is the common shear modulus of the two phases (the elastic con-

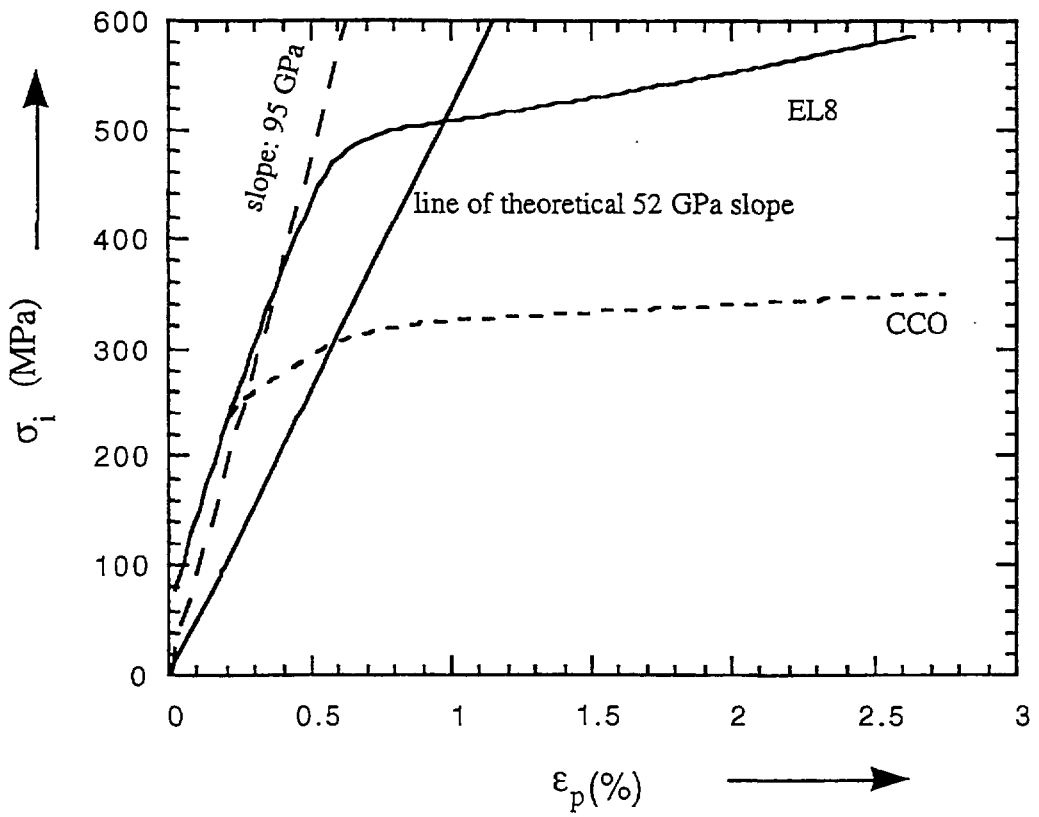

Fig. 8. Experimental and theoretical internal stress variation with ε_p

stants of the matrix and of hard phase are roughly the same), f is the volume fraction of the hard phase, γ is a dimensionless parameter which takes into account the shape of particles. For this estimation the austenite/ferrite system is considered as a matrix/fibre composite where fibres are parallel to the tensile axis. As the two phases are percolated they have the same overall deformation. This situation is therefore similar to a parallel loading of the two phases. In this case one gets $\gamma \approx 0.69$ (multiple slip). In the original model the volume fraction of inclusions is small so that the proportion of matrix is close to unity. Here, for a volume fraction of ferrite $f_{ferr} = 0.33$, it is necessary to take into account $1 - f_{ferr}$. Equation (6) becomes (7)

$$\sigma_i = 2\gamma\mu\varepsilon_p \frac{f_{ferr}}{1 - f_{ferr}} ; \tag{7}$$

from which the theoretical slope $d\sigma_i/d\varepsilon_p$ is 52 GPa. This value is lower than but of the same order as the experimental slope which is 95 GPa (Fig. 8). This slight discrepancy can probably be related to the complex topology of the ferrite/austenite mixture. It is worth noticing that if instead of $f_{ferr} = 0.33$ we had taken $f_{ferr} = 0.48$, the slope would have been of 95 GPa: it seems then that the material behaves as if the effective volume fraction of ferrite was larger than the real volume fraction which could come from the existence of "constrained austenite" unable to deform plastically.

5.3 Local stresses in ferrite

At the transition point the internal stresses in austenite are of the order of 300 MPa for CC0 and 500 MPa for aged materials. Local stresses in the ferritic phase are calculated using a stress equilibrium equation [5],

$$\sigma_{ferr} f_{ferr} + \sigma_i (1 - f_{ferr}) = 0 . \tag{8}$$

Estimating σ_{ferr} using the effective volume fraction of ferrite $\bar{f}_{ferr}$ leads to

- $\sigma_{ferr} \approx 325$ MPa for CC0 ,
- $\sigma_{ferr} \approx 540$ MPa for aged states .

These values are comparable to the yield stresses of ferrite in both CC0 and CC7 heat treatments. When plasticity in ferrite occurs (see Table 3), further deformation is possible without increasing anymore the internal stresses: this is the reason for the transition in slope in Fig. 8.

5.4 Internal stresses for $\varepsilon_p = 0$

The origin of internal stresses pre-existing to any deformation (at $\varepsilon_p = 0$) can be due to the difference between the lattice parameters (σ_{para}) and thermal expansion coefficients (σ_{th}) of the two phases. Some compression–tension tests were carried out in association with tension–compression tests in order to estimate the importance of these stresses. As noticed in Table 4, the tension–compression and the compression–tension test experiments at the same total prestrains (the plastic prestrains are roughly the same) lead to the same value of internal stresses, $\Delta\sigma_t$ (tension–compression test) $\approx \Delta\sigma_c$ (compression–tension test). As $\sigma_{th} - \sigma_{para} = (1/4)\ (\Delta\sigma_c - \Delta\sigma_t)$ [10], the stresses due to the misfit and the difference of thermal coefficients between the two phases are totally relaxed.

6. Conclusion

The internal stresses in deformed austenoferritic duplex stainless steels are extremely large. The homogeneous plastic deformation in the non-aged material and the localized glide in the aged material allow the internal stresses to be partly relaxed. Cleavage of aged ferrite is not responsible for this relaxation since ferrite cleaves without decohesion and the interface still contributes to the load transfer between the two phases.

The comparison between the theoretical calculation of internal stress accumulation for low plastic strains and experimental results show that the effective proportion of ferrite is larger than the real ferrite volume fraction. This suggests that a fraction of austenite can be embedded in ferrite and therefore does not undergo plastic deformation.

The stresses coming from the lattice misfit and the difference of the thermal expansion coefficients are fully relaxed.

Acknowledgements The authors are indebted to Prof. J. D. Embury for stimulating discussions, to Mr. D. Teulet for help in the Bauschinger experiments and to "Electricité de France" for financial support.

References

[1] M. F. Ashby, Phil. Mag. **21**, 399 (1970).
[2] E. Orowan, Symp. Internal Stresses and Fatigue in Metals, Elsevier Publ. Co., New York 1959.
[3] P. S. Bate and D. V. Wilson, Acta metall. **34**, 1097 (1986).
[4] D. V. Wilson and P. S. Bate, Scripta metall. **20**, 1529 (1986).
[5] J. D. Embury, Mater. Forum **10**, 27 (1987).
[6] A. Abel, Mater. Forum **10**, 11 (1987).
[7] J. Gerbase, J. D. Embury, and R. M. Hobbs, Structure and Properties of Dual-Phase Steels, MS AIME, New Orleans 1979 (p. 118).
[8] L. M. Brown and D. R. Clarke, Acta metall. **23**, 821 (1975).
[9] L. M. Brown, Scripta metall. **11**, 127 (1977).
[10] Y. Bréchet and P. Jarry, J. Physique (III) **1**, 1985 (1991).
[11] S. Bonnet, J. Bourgoin, J. Champredonde, D. Guttmann, and M. Guttmann, Mater. Sci. Technol. **6**, 221 (1990).
[12] O. K. Chopra and H. M. Chung, PVP ASME **132**, 79 (1988).
[13] P. Joly and A. Pineau, 32ème Colloque Métallurgie de Saclay, INSTN Saclay, Ed. Revue de Métallurgie, 1989 (p. 49).
[14] P. Auger, F. Danoix, A. Menand, S. Bonnet, J. Bourgoin, and M. Guttmann, Mater. Sci. Technol. **6**, 301 (1990).
[15] M. Guttmann, Duplex stainless steels '91, Beaune (Bourgogne, France), Ed. J. Charles and S. Bernhardsson, Les Editions de Physique, 1991 (p. 79).

EDF
Electricité de France

Direction des Etudes et Recherches

Service Information Prospective et Normalisation

Département Systèmes d'information et de documentation

Groupe Exploitation de la Documentation Automatisée

1, avenue du Gal de Gaulle
92141 CLAMART Cedex
tel : 47 65 56 33

CLAMART Le 27/05/97

MME AUBRY JACQUELINE
CEA - CE SACLAY
DIST/SCIBD
ORNE DES MERISIERS

91191 GIF SUR YVETTE CEDEX

à l'attention de :

MEMOIRE TECHNIQUE ELECTRONIQUE

****
Cette feuille est détachable grâce à la microperforation sur le coté droit.
****

Référence de la demande : **F619031** Votre commande : **DIST/SCIBD/97/003**
Origine : **CATALOGUE DES NOTES DER**

Numéro du document : **96NB00143**

Titre : **DETERMINATION DES CONTRAINTES INTERNES DANS UN ACIER INOXYDABLE AUSTENOFERRITIQUE**

Auteurs : **VERHAEGHE B./BRECHET Y./LOUCHET F./MASSOUD J.P./TOUZEAU D.**

Source : **COLL. NOTES INTERNES DER. PRODUCTION D'ENERGIE (HYDRAULIQUE, THE**
Serial :

Référence du document : **SANS**

Nombre de pages: **0014** Nombre d'exemplaires : **001** Support : **P**